Electronic Supplementary Material (ESI) for Inorganic Chemistry Frontiers.

Supporting Information

Regulating the Lattice Strain of Platinum-Copper Catalysts for Enhancing Collaborative Electrocatalysis

Fangfang Chang[a], Yongpeng Liu [a], Qing Zhang[a], Zhichao Jia[a], Xiaolei Wang[b], Lin Yang[a]* and Zhengyu Bai[a]*

[a] Collaborative Innovation Center of Henan Province for Green Manufacturing of Fine Chemicals, Key Laboratory of Green Chemical Media and Reactions, Ministry of Education, School of Chemistry and Chemical Engineering, Henan Normal University, Xinxiang, Henan 453007, China. Email: yanglin@htu.edu.cn; baizhengyu@htu.edu.cn
[b]Department of Chemical and Materials Engineering, University of Alberta, Edmonton, Alberta T6G 1H9, Canada.

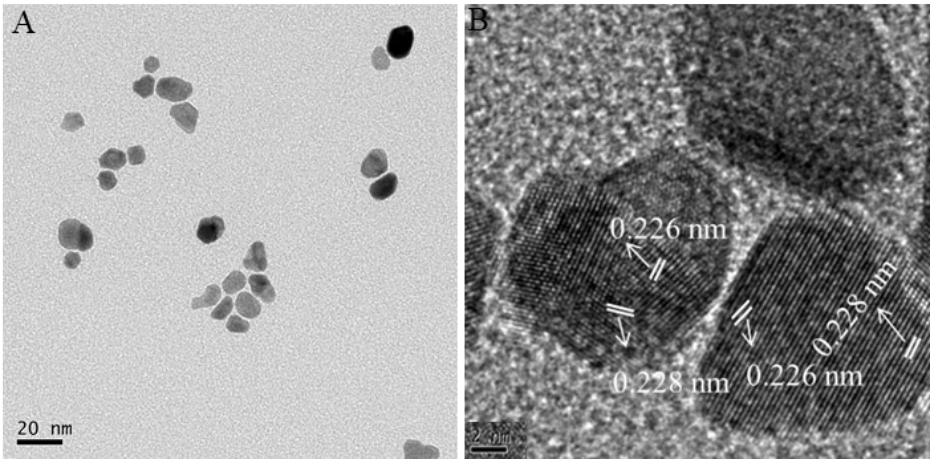

Figure S1. TEM (A) and HR-TEM (B) images of Pt NPs with 11.2±1.4 nm size

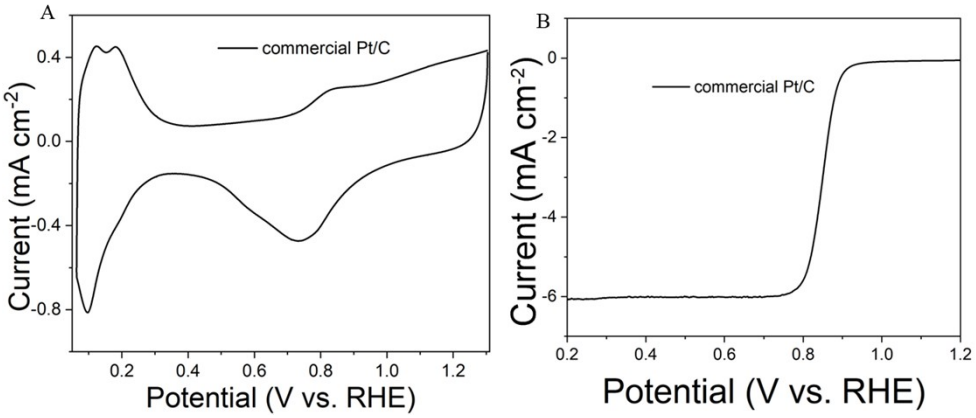

Figure S2. (A) CV and (B) RDE curves for commercial Pt/C in 0.1 M HClO4 solution saturated with nitrogen (scan rate: 50 mV/s) and oxygen (scan rate: 10 mV/s and rotation speed: 1600 rpm)

Table S1. Summary of physical and ORR data for Pt-Cu NPs/C catalysts

Catalysts	NWs size on carbon (nm)	Metal loading (%wt)	ECSA (m^2/g_{Pt})	Mass activity (A/mg_{Pt}^{-1})	Specific activity (mA/cm^2)
$Pt_{10}Cu_{90}/C$	9.5±2.5	20.00%	47	0.35	0.74
$Pt_{42}Cu_{58}/C$	9.0±1.3	20.00%	63	0.82	1.3
$Pt_{69}Cu_{31}/C$	9.7±1.8	22.00%	87	1.23	1.41
Pt NPs/C	11.2±1.4	13.00%	70.1	0.42	0.6
Commercial Pt/C	2.3±0.6	20.00%	62.5	0.21	0.34

Table S2. Comparison of ORR activities of various catalysts

Catalyst	Mass activity (A/mg_{Pt}^{-1})	Specific activity (mA/cm^2)	Reference
Annealed Pt-Cu NPs	0.14	0.75	1
PtCu5@Pt/C	0.17	0.36	2
$Pt_{75}Cu_{25}/C$	0.38	0.69	3
FePtCu nanorods	0.22	0.33	4
PtCu nanoframes	0.82	1.24	5
commercial Pt/C	0.21	0.34	**This work**
$Pt_{69}Cu_{31}/C$	**1.23**	**1.41**	**This work**

Table S3. Summary of physical and MOR data for Pt-Cu NPs/C catalysts

Catalysts	Metal loading (% wt)	Mass activity (A/mg_{Pt}^{-1})	Specific activity (mA/cm^2)
$Pt_{10}Cu_{90}/C$	20.00%	0.46	0.98
$Pt_{42}Cu_{58}/C$	20.00%	1.32	2.1
$Pt_{69}Cu_{31}/C$	22.00%	2.13	2.45
Pt NPs/C	13.00%	0.78	1.11
commercial Pt/C	20.00%	0.54	0.86

Table S4. Comparison of MOR activities of various catalysts

Catalyst	Electrolyte	Mass activity (A/mg_{Pt}^{-1})	Specific activity (mA/cm^2)	Reference
Hollow Pt-Cu alloy tetradecahedrons	0.5 M H_2SO_4 + 1 M Methanol	0.88		6
Hollow PtCu/C	0.5 M H_2SO_4 + 0.5 M methanol	0.889	1.77	7
Porous PtCu nanocrystals	0.1 M $HClO_4$+0.2 M Methanol	1.55	2.88	8
PtCu nanodendrites	0.1 M $HClO_4$+1 M Methanol	1	1.04	9
$Pt_{42}Cu_{58}$/C	0.1 M $HClO_4$+0.5 M Methanol	1.32	2.1	**This work**
$Pt_{69}Cu_{31}$/C	0.1 M $HClO_4$+0.5 M Methanol	2.13	2.45	**This work**

Table S5. Summary of physical and EOR data for Pt-Cu NPs/C catalysts

Catalysts	Metal loading (% wt)	Mass activity (A/mg_{Pt}^{-1})	Specific activity (mA/cm^2)
$Pt_{10}Cu_{90}$/C	20.00%	0.29	0.62
$Pt_{42}Cu_{58}$/C	20.00%	0.96	1.52
$Pt_{69}Cu_{31}$/C	22.00%	1.08	1.24
Pt NPs/C	13.00%	0.55	0.78
commercial Pt/C	20.00%	0.23	0.37

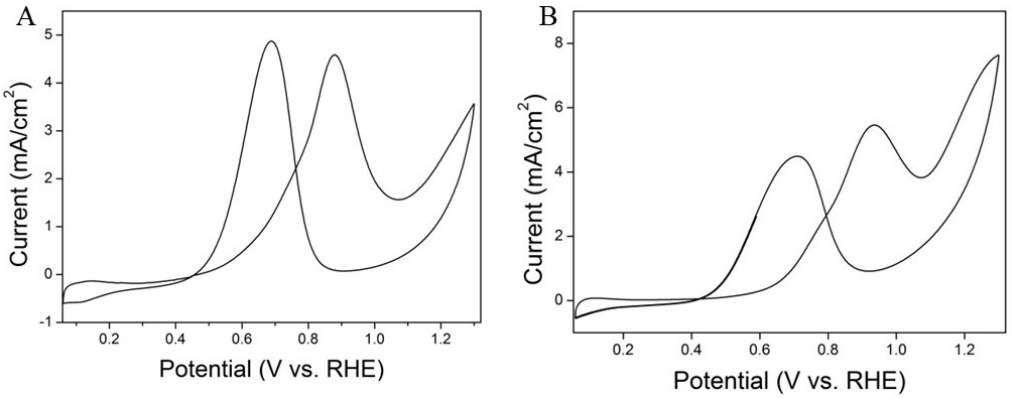

Figure S3 (A) CV curve of commercial Pt/C in 0.1 M $HClO_4$ + 0.5 M CH_3OH solution purged with N_2 at a scan rate of 50 mV s^{-1}; (B) CV curves of commercial Pt/C in 0.1 M $HClO_4$ + 0.5 M C_2H_5OH solution purged with N_2 at a scan rate of 50 mV s^{-1}

Table S6. Comparison of EOR activities of various catalysts

Catalyst	Electrolyte	Mass activity (A/mg_{Pt}^{-1})	Specific activity (mA/cm^2)	Reference
Sub-5.0 nm PtCu nanoalloys	0.5 M KOH + 0.5 M Ethanol	0.81		10
$Pt_{34}Pd_{33}Cu_{33}$	0.1MHClO4+0.5M Ethanol	0.19	1.13	11
3D hierarchical PtCu	0.5 M KOH + 2.0 M ethanol	0.4		12
PtAu alloyed nanoflowers	1.0 M KOH + 0.5 M ethanol	0.95		13
Pt-Cu/RGO	0.5 M H_2SO_4 + 0.5 M Ethanol	0.53		14
$Pt_{42}Cu_{58}$/C	0.1 M $HClO_4$+0.5 M Ethanol	0.96	1.52	**This work**
$Pt_{69}Cu_{31}$/C	0.1 M $HClO_4$+0.5 M Ethanol	1.08	1.24	**This work**

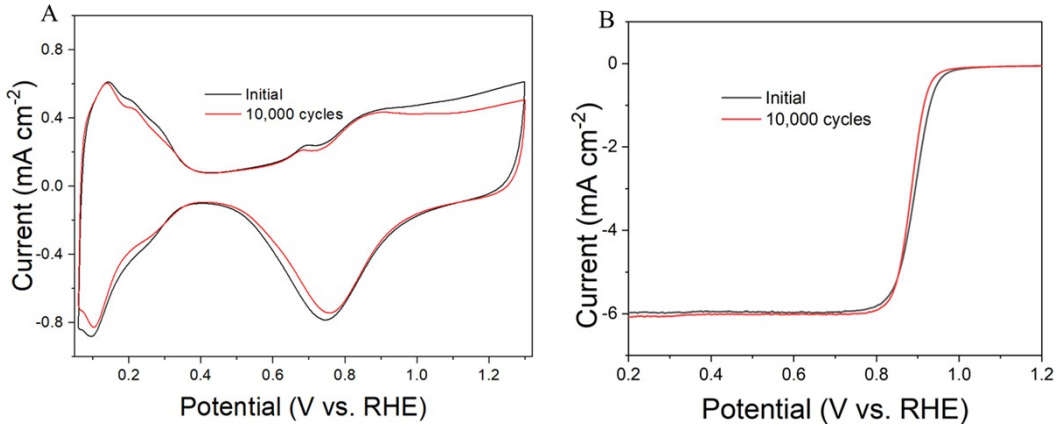

Figure S4. (A) CV and (B) RDE curves for commercial Pt/C before and after 10,000 potential cycles (sweep rate, 100mV/s, potential cycle window: 0.6 and 1.1 V) in 0.1 M $HClO_4$ solution saturated with nitrogen (scan rate: 50 mV/s) and oxygen (scan rate: 10 mV/s and rotation speed: 1600 rpm).

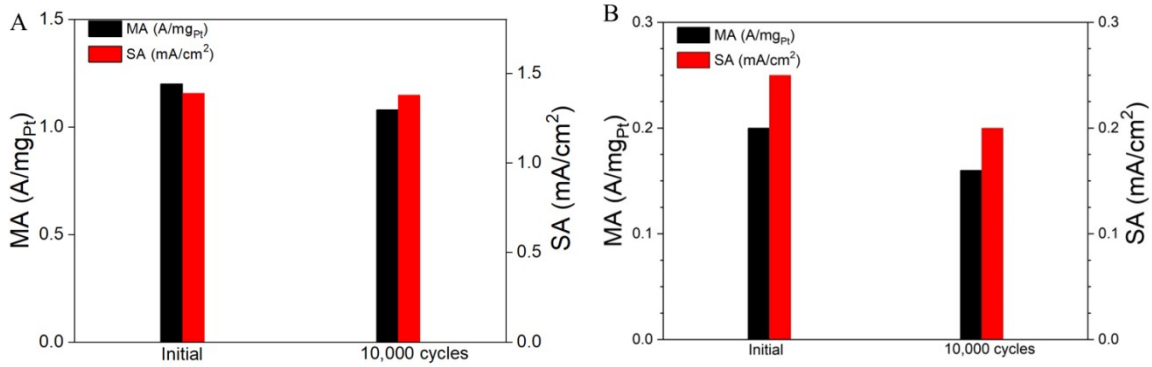

Figure S5. Mass activity and specific activity data (A) $Pt_{69}Cu_{31}$/C NWs and (B) commercial Pt/C at 0.900 V (vs. RHE) before and after 10,000 cycles.

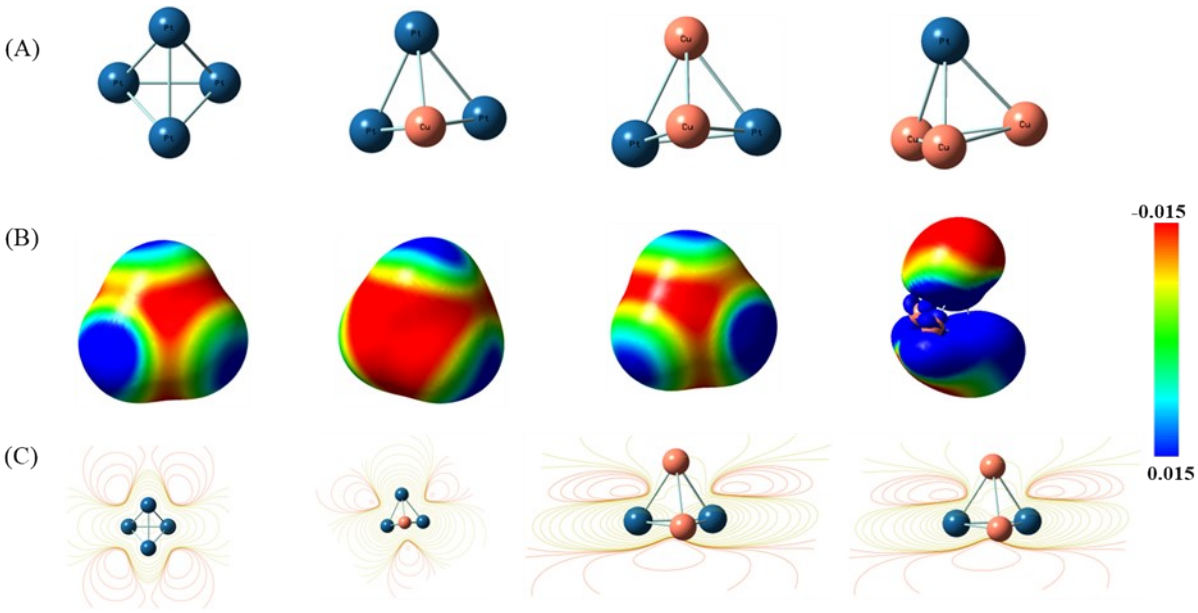

Figure S6. (A) Optimized geometric structure (B) isosurface map and (C) contour map of electrostatic surface potential (ESP) of Pt_xCu_{4-x} (x =4, 3, 2, 1) clusters by DFT calculation. The calculations used Gaussian 09 and GaussView 5.0, with a model of 4-atom Pt-Cu cluster, involving Optimization; Method via B3LYP functional with LanL2DZ basis set was used to obtain electronic properties and molecular orbitals.

Table S7. The electron configuration and natural atomic charge of the optimized structure of Pt_xCu_{4-x} (x=1, 2, 3, 4) clusters

cluster	atom No	electron configuration	charge	e-transfer
Pt_4	1Pt	$6S^{0.57}5d^{9.41}6p^{0.08}$	0.00	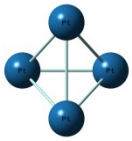
	2Pt	$6S^{0.057}5d^{9.41}6p^{0.08}$	0.00	
	3Pt	$6S^{0.057}5d^{9.41}6p^{0.08}$	0.00	
	4Pt	$6S^{0.057}5d^{9.41}6p^{0.08}$	0.00	
Pt_3Cu_1	1Cu	$4S^{0.21}3d^{4.97}4p^{0.08}$	0.438	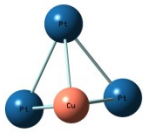
	2Pt	$6S^{0.32}5d^{4.89}6p^{0.04}$	-0.146	
	3Pt	$6S^{0.32}5d^{4.89}6p^{0.04}$	-0.146	
	4Pt	$6S^{0.32}5d^{4.89}6p^{0.04}$	-0.146	
Pt_2Cu_2	1Cu	$4S^{0.82}3d^{9.77}4p^{0.24}5S^{0.01}$	0.167	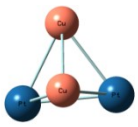
	2Pt	$6S^{0.89}5d^{9.00}6p^{0.28}$	-0.167	
	3Pt	$6S^{0.89}5d^{9.00}6p^{0.28}$	-0.168	
	4Cu	$4S^{0.82}3d^{9.77}4p^{0.24}5S^{0.01}$	0.168	
Pt_1Cu_3	1Cu	$4S^{0.60}3d^{9.93}4p^{0.28}$	0.190	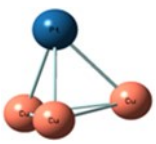
	2Pt	$6S^{1.48}5d^{8.82}6p^{0.19}7S^{0.01}7p^{0.01}$	-0.499	
	3Cu	$4S^{0.58}3d^{9.93}4p^{0.28}$	0.203	
	4Cu	$4S^{0.73}3d^{9.90}4p^{0.25}$	0.106	

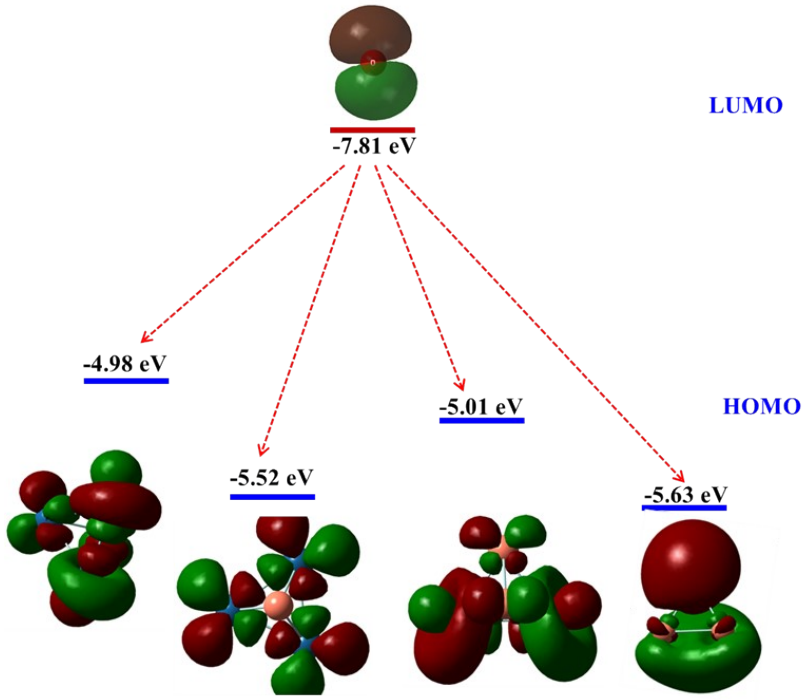

Figure S7. Frontier molecular orbitals and the energy of LUMO of O atom and HOMO of Pt_xCu_{4-x} (x = 4, 3, 2, 1) clusters

Table S8. Structure and binding energy ((eV) for Pt_xCu_{10-x} (x=1, 4, 7, 10) clusters

Pt_1Cu_9	Pt_4Cu_6	Pt_7Cu_3	Pt_{10}
	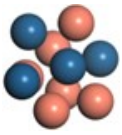	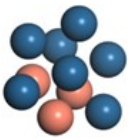	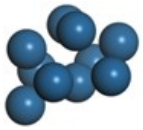
1.69	1.52	1.75	2.20

Table S9. Structure and adsorption energy (eV) for O on Pt_xCu_{10-x} (x=1, 4, 7, 10) clusters

	Pt_1Cu_9	Pt_4Cu_6	Pt_7Cu_3	Pt_{10}
	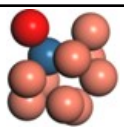	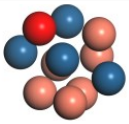	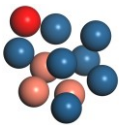	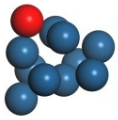
O	6.88	5.03	4.79	4.53

Table S10. Structure and adsorption energy (eV) for OOH on Pt_xCu_{10-x} (x=1, 4, 7, 10) clusters

	Pt_1Cu_9	Pt_4Cu_6	Pt_7Cu_3	Pt_{10}
	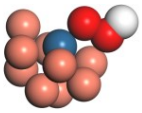	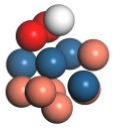	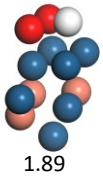	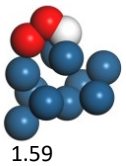
OOH	5.90	1.96	1.89	1.59

Table S11. Structure and adsorption energy (eV) for OH on Pt_xCu_{10-x} (x=1, 4, 7, 10) clusters

	Pt_1Cu_9	Pt_4Cu_6	Pt_7Cu_3	Pt_{10}
	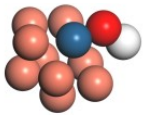	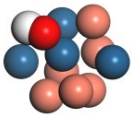		
OH	4.11	2.65	2.56	2.41

Table S12. Structure and adsorption energy (eV) for CO on Pt_xCu_{10-x} (x=1, 4, 7, 10) clusters

	Pt_1Cu_9	Pt_4Cu_6	Pt_7Cu_3	Pt_{10}
	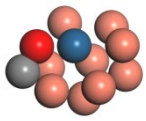	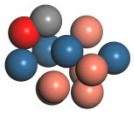	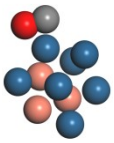	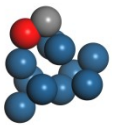
CO	1.69	1.52	0.353	2.20

Table S13. The correction of zero point energy and entropy of the adsorbed and gaseous species.

	ZPE(eV)	TS(eV)
*OOH	0.35	0
*O	0.05	0
*OH	0.31	0.01
H_2O	0.56	0.67
H_2	0.27	0.41

References

1 D. Indrajit, K. -C. Michael, P. -B. Michael, M. -Z. Joseph, E. -M. Thomas, H. -A. Mohammed, P. -I. Nicholas, Electrochemical and structural study of a chemically dealloyed PtCu oxygen reduction catalyst, *J. Phys. Chem. C*., 2010, **114**, 16309-16320.

2 J. Namgee, S. Yeonsun, H. -P. Jin, S. -N. Kee, K. Pil, Y. Sung Jong, High-performance PtCux@Pt core-shell nanoparticles decorated with nanoporous Pt surfaces for oxygen reduction reaction, *Appl. Catal. B-Environ*., 2016, **196**, 199-206.

3 Y. Liu, L. Chen, T. Cheng, H. Guo, B. Sun, Y. Wang, Preparation and application in assembling high-performance fuel cell catalysts of colloidal PtCu alloy nanoclusters, *J. Power. Sources*., 2018, **395**, 66–76.

4 H. Zhu, S. Zhang, S. Guo, D. Su, S. Sun, Synthetic control of FePtM nanorods (M = Cu, Ni) to enhance the oxygen reduction reaction, *J. Am. Chem. Soc*., 2013, **135**, 7130-7133.

5 M. Gong, D. Xiao, Z. Deng, R. Zhang, D. Wang, Structure evolution of PtCu nanoframes from disordered to ordered for the oxygen reduction reaction, *Appl Catal B-Environ*., 2021, **282**, 119617.

6 R. Zhao, G. Fu, Z. Chen, Y. Tang, Y. Wang, S. Huang, A novel strategy for the synthesis of hollow Pt–Cu tetradecahedrons as an efficient electrocatalyst toward methanol oxidation, *CrystEngComm*., 2019, **21**, 1903–1909.

7 X. Huang, C. Yu, E. Zhu, Y. Xu, X. Duan, H. Yu, Monodisperse Cu@PtCu nanocrystals and their conversion into hollow-PtCu nanostructures for methanol oxidation, *J. Mater. Chem. A*., 2013, **1**, 14449–14454.

8 K. Eid, H. Wang, P. He, K. Wang, T. Ahamad, S. M. Alshehri, Y. Yamauch, L. Wang, One-step synthesis of porous bimetallic PtCu nanocrystals with high electrocatalytic activity for methanol oxidation reaction, *Nanoscale*., 2015, **7**, 16860–16866.

9 L. Guo, L. -B. Huang, W. -J. Jiang, Z. Wei, Tuning the branches and composition of PtCu nanodendrites through underpotential deposition of Cu towards advanced electrocatalytic activity, *J. Mater. Chem. A*., 2017, **5**, 9014–9021.

10 T. Liu, W. Kai, Y. Qiang, Z. Shen, W. Ye, Q. Zhang, Monodispersed sub-5.0 nm PtCu nanoalloys as enhanced bifunctional electrocatalysts for oxygen reduction reaction and ethanol oxidation reaction, *Nanoscale*., 2017, **9**, 2963–2968.

11 J. Lan, K. Wang, Q. Yuan, X. Wang, Composition-controllable synthesis of defect-rich PtPdCu nanoalloys with hollow cavities as superior electrocatalysts for alcohol oxidation, *Mater. Chem. Front*., 2017, **1**, 1217-1222.

12 F. Nosheen, Z. -C. Zhang, G. -L. Xiang, B. Xu, Y. Yang, F. Saleem, X. -B. Xu, J. -C. Zhang, X. Wang, Three-dimensional hierarchical Pt-Cu superstructures, *Nano Res*., 2015, **8**, 832-838.

13 P. Song, L. -P. Mei, A.- J. Wang, K. -M. Fang, J. -J. Feng, One-pot surfactant-free synthesis of porous PtAu alloyed nanoflowers with enhanced electrocatalytic activity for ethanol oxidation and oxygen reduction reactions, *Int. J. Hydrogen Energy*., 2016, **41**, 1645-1653.

14 T. Liu, C. Li, Q. Yuan, Facile synthesis of PtCu alloy/graphene oxide hybrids as improved electrocatalysts for alkaline fuel cells, *ACS. Omega*., 2018, **3**, 8724−8732.